Monitoring the immune responses to vaccination and pertussis: bordetella pertussis and beyond

Diks, A.M.

Chapter 4

PLCG2 variant p.P522R -associated with healthy aging- may reduce the aging of the human immune system

A.M. Diks[1 2], C. Teodosio[1 3], B. De Mooij[1], R.J. Groenland[1], B.A.E. Naber[1], I.F. de Laat[1], A.A. Vloemans[1], S. Rohde[2], M.I. de Jonge[4], L. Lorenz[2], D. Horsten[2], J.J.M. van Dongen[1 3], M.A. Berkowska[1*], H. Holstege[2*]

[1] Department of Immunology, Leiden University Medical Center, Albinusdreef 2, 2333 ZA, Leiden, the Netherlands
[2] Department of Human Genetics, Vrije Universiteit Amsterdam, Amsterdam UMC, Amsterdam, the Netherlands
[3] Translational and Clinical Research Program, Cancer Research Center (IBMCC; University of Salamanca - CSIC); Cytometry Service, NUCLEUS; Department of Medicine, University of Salamanca and Institute of Biomedical Research of Salamanca (IBSAL), Spain
[4] Laboratory of Medical Immunology, Radboud Institute for Molecular Life Sciences, Radboud University Medical Centre, Nijmegen, The Netherlands

* These authors contributed equally to this manuscript

Manuscript submitted

Abstract

Background: Phospholipase C gamma 2 (PLCγ2) is encoded by the *PLCG2* gene. A single-nucleotide polymorphism (p.P522R) associates with protection against several dementia subtypes and with increased likelihood of longevity. Cell lines and animal models indicated that p.P522R is a functional hypermorph. We aimed to confirm this in human peripheral immune cells.

Methods: We compared effects of p.P522R on immune system function between carriers and non-carriers (aged 59-103y), using in-depth immunophenotyping, functional B-cell and myeloid-cell assays, and *in vivo* SARS-CoV-2 vaccination.

Results: As expected, effects of p.P522R on immune cell function were small. Immune cell numbers in p.P522R carriers better resembled a younger reference cohort than those of non-carriers. Moreover, carriers expressed lower levels of FcεRI on several immune cell subsets and elevated CD33 levels on classical monocytes. Upon B-cell stimulation, PLCγ2 phosphorylation and calcium release were increased in carriers compared to non-carriers. Normalized ROS production in myeloid cells was higher upon PLCγ2-dependent stimulation, but lower upon PLCγ2-independent stimulation. Carriers and non-carriers had similar serological responses to SARS-CoV-2 vaccination.

Conclusion: Compared to non-carriers, immune profiles from carriers more closely resembled those from younger individuals, suggesting that p.P522R associates with resilience against immunological aging.

Keywords: Phospholipase C gamma 2, PLCγ2 p.P522R, *PLCG2* rs72824905, healthy aging, immunosenescence, flow cytometry, functional studies

Background

The average human lifespan has greatly expanded in the past decennia. In most individuals, increase in age coincides with a decline in cognitive and physical health. Many age-related impairments, such as lowered resistance to infection, dementia, osteoporosis, atherosclerosis, and diabetes are directly or indirectly related to the aging immune system, especially to the low grade inflammation that is frequently observed in older individuals (inflamm-aging).(1, 2)

Upon aging, the output of naive B and T cells from the bone marrow into the periphery decreases, leading to lower numbers of naive lymphocytes in the circulation. Additionally, B and T-cell receptor (BCR, TCR) diversity decreases upon aging, leaving aged individuals less equipped to deal with neo-antigens.(1, 3, 4) Human and animal models have shown impaired germinal center (GC) formation, reduced affinity maturation, reduced memory B-cell (MBC) differentiation and lowered levels of plasma cells in the bone marrow.(3) Additionally, the functioning of innate immune cells declines. In neutrophils derived from aged individuals, a lowered capacity to phagocytose opsonized particles and decreased production of reactive oxygen species (ROS) was reported.(4, 5) Likewise, monocytes derived from older adults showed reduced phagocytic capacity, lowered ROS production and lower anti-tumor properties.(1, 6, 7)

Each individual is uniquely vulnerable to the effects of aging. Therefore, several studies have searched for (biomolecular) elements and pathways associated with resilience to the effects of aging, i.e. that optimally maintain both physical and cognitive functions during the aging process.(8-10) One of the factors identified is a single-nucleotide polymorphism (SNP) in the Phospholipase C gamma 2 (*PLCG2*) gene (p.P522R, rs72824905).(8)

PLCγ2 is an enzyme with a critical regulatory role in various immune and inflammatory pathways. It is involved in downstream receptor signaling where, upon receptor stimulation, it hydrolyses PIP2 (phosphatidylinositol 4,5-bisphosphate) to generate IP3 (inositol 1,4,5-triphosphate) and DAG (diacylglycerol), which are second messenger molecules that further transmit the activation signal, leading to the release of intracellular calcium.(11, 12) Amongst others, PCLγ2 is expressed downstream of several members of the immunoglobulin superfamily, such as the B-cell receptor on B cells, but also downstream of Fc receptors (FcR) in innate cells, such as FcRγIII and 2B4 on NK cells, FcεRI on mast cells, TREM (Triggering Receptors Expressed on Myeloid cells) on macrophages and microglia, and FcR-involving collagen receptors on platelets.(12-14)

We previously observed that the p.P522R variant was associated with a lower risk of several forms of age-related neurodegenerative diseases, including Alzheimer's disease, frontotemporal dementia, dementia with Lewy Bodies, and progressive supranuclear palsy.(9, 15) Recently, multiple sclerosis was added to this list.(16) This p.P522R variant simultaneously associates with increased likelihood of ex-

treme longevity.(9) In fact, a recent study suggested that the p.P522R variant may maintain cognitive function during aging by mitigating the accumulation of toxic tau pathology in the brain, when this co-occurs with the accumulation of amyloid pathology, both hallmarks of Alzheimer's disease.(17) The same study suggested that the cognitive decline observed in individuals who carry the APOE-ε4 allele, the strongest genetic risk factor for Alzheimer's disease, in combination with the p.P522R *PLCG2* variant, was slower and less compared to individuals who carried the APOE-ε4 allele without the protective p.P522R variant.(9, 17) Together, this suggests that the effect of p.P522R associates with maintaining an aspect of the immune system that, when compromised, increases the risk of these neurodegenerative diseases. Many studies have therefore investigated the effect of this variant in the innate immune cells of the brain, the microglia. However, *PLCG2* is most prominently expressed in peripheral immune cells, suggesting that this variant may also affect human peripheral immune system function. Furthermore, it might well be that the peripheral immune system function also influences brain function.

The p.P522R variant was shown to be a gain-of-function variant (functional hypermorph) in transfected COS7, HEK239T and BV2 cells, a p.P522R mouse model, and gene-edited human iPSCs.(13, 18, 19) In the current study, we investigated the impact of p.P522R carriership on the human immune system and its implications for healthy aging. To the best of our knowledge, an in-depth evaluation of the PLCγ2 expression in circulating immune cells between p.P522R carriers and non-carriers has not yet been performed. We hypothesized that the immune system of p.P522R carriers translates to an increased resilience to the effects of aging compared to age-matched non-carriers. To this end, we investigated the quantities, immunophenotypes, and functions of circulating immune cells in p.P522R carriers and non-carriers from 9 different nuclear families, in which one parent reached 100 years with high levels of cognitive performance and carried the p.P522R variant. We evaluated phosphorylation of PLCγ2 and calcium release upon BCR stimulation and analyzed the replication history in B-cell subsets. *In vivo* B-cell responses were assessed by measuring the serum Ig response to SARS-CoV-2 vaccination. Lastly, myeloid cell subsets were exposed to opsonized Escherichia coli, after which phagocytosis and ROS production were monitored.

Methods

Experimental design

A total of 36 individuals from the 100 plus study cohort, as previously described by Holstege et al (20), were selected for this study (METC number: 2016.440, approved by the Medical Ethics Committee of the VU University Medical Center, Amsterdam, the Netherlands). In short, volunteers either had to be ≥100 years, and self-reported as cognitively healthy, which was confirmed by a family member of close relation (20), or to be the offspring or a sibling of such individuals. When including offspring, the parent had to be a confirmed p.P522R carrier. After inclusion, peripheral blood (PB) was collected at one or multiple

occasions in K3EDTA collection tubes (PB-EDTA), sodium heparin collection tubes (PB-HEP), and serum collection tubes (BD Vacutainer, BD Biosciences, San Jose, Ca, USA). To avoid influence of circadian rhythm on cell counts, samples were always collected in the morning. p.P522R carriership was determined by Sanger sequencing or Illumina Genome Screening Array (GSA, GSAshared-CUSTOM_20018389_A2, v1, human genome build 37) as described elsewhere.(21) In the current study, we investigated quantities, immunophenotypes, and functions of circulating immune cells in three overlapping cohorts (Cohort I, II and III), described in **Table 1**. Immunophenotyping was performed on all individuals included in Cohort I (n=33). Calcium flux measurements were performed on cells from donors included in Cohort I and II, with exception of two donors that showed B-cell aberrancies (n=33). Functional evaluation (phosphorylation of PLCγ2, KREC analysis, phagocytosis assay and ROS production) was performed on Cohort II (n=14). Lastly, vaccination responses were evaluated in Cohort III (n=22). Family composition can be found in **Table S1**.

Settings of flow cytometers

For all flow cytometers (available at the Flow cytometry Core Facility at LUMC) there was a daily quality control (QC). QC for Cytek Aurora flow cytometers (Cytek Biosciences, Fremont, Ca, USA) was performed using SpectroFlo QC Beads (Cytek Biosciences). BD FACS LSR Fortessa 4L and BD FACS Canto II 3L (BD Biosciences, San Jose, CA, USA) were calibrated according to EuroFlow guidelines and daily QC was performed using BD™ Setup and Tracking (CS&T) beads (BD Biosciences) and Perfect-Count Microspheres™ (Cytognos, Spain), as described before.(22, 23)

Immunophenotyping of circulating immune cells

PB-EDTA from Cohort I was used <12h after collection for immunophenotyping. In-depth analysis of circulating innate and adaptive immune cells was performed using previously published flow cytometry panels, or their direct prototypes, and gating strategies (**Table S2**).

The dendritic cell-monocyte (DC-monocyte) panel allows identification of up to 19 different (sub)populations in the myeloid compartment.(24, 25) The CD4-T cell panel (CD4T) allows identification of at least 89 (sub)populations within the CD4 T-cell compartment, which comprise of different functionalities and maturation stages.(25, 26) The CD8 cytotoxic T-cell (CYTOX) panel allows identification of up to 50 (sub)populations within the CD8 T-cell and the natural killer (NK) cell compartments.(25) Lastly, the B-cell and plasma cell (BIGH) panel allows identification of up to 115 populations of B and plasma cells, distinguished based on their maturation stage-associated phenotype and the expressed Ig subclasses.(25, 27, 28)

Depending on the antibody combination, samples were either processed according to the bulk lysis protocol for staining of 10 x 10^6 cells (DC-monocyte and BIGH) or prepared using the EuroFlow stain-lyse-wash protocol (CD4T,

CYTOX); both protocols available on www.EuroFlow.org. For BIGH and CYTOX tubes, surface staining was followed by intracellular staining with the Fix & Perm reagent kit (Nordic MUbio, Susteren, The Netherlands) according to manufacturer's protocol. In brief, 100µl of washed sample was fixed with 100µl of Solution A (15 min in the dark at RT), washed, and permeabilized by adding 100µl of Solution B (15 min in the dark at RT) and antibodies against intracellular markers. After washing, cells were re-suspended in PBS for immediate acquisition (or stored for max ~3h at 4◦C).

Table 1. Description of the cohorts used in this study; Cohort I, II, III.

Cohort I: Extensive immunophenotyping			
	Min-max age	**Mean/median age**	**M/F**
Carriers (18)	59-103 y	75. 1/71 y	7/11
Non-carriers (15)	61-83 y	73.1/74 y	8/7

- Cognitively healthy individuals
- p.P522R carrying centenarian; or a child/sibling of such centenarian
- 33 donors from 7 families
  - Blood collection
  - Immunophenotyping of >100 circulating immune cell subsets
  - PBMCs storage

Cohort II: Functional assays			
	Min-max age	**Mean/median age**	**M/F**
Carriers (8)	59-78 y	69.5/69 y	6/2
Non-carriers (6)	71-83 y	77.3/77.5y	4/2

- Healthy individuals (based on clinical records and current medication use)
- 14 donors from 8 families (12/14 donors selected from Cohort I)
  - Blood collection for:
    - B-cell activation
    - Replication history of B-cell subsets
    - Phagocytic capacity

Cohort III: *in vivo* evaluation			
	Min-max age	**Mean/median age**	**M/F**
Carriers (10)	62-82 y	73.1/71.5 y	6/4
Non-carriers (12)	64-87 y	76.3/76.5y	8/4

- Vaccinated against SARS-CoV-2
- 22 donors from 9 families (entire cohort II + 7 donors from Cohort I + 1 additional donor)
  - Serum collection 7-14 weeks after second vaccination
    - Detection of serum IgG, IgA and IgM responses against:
      - Receptor Binding Domain
      - Spike protein
      - Nucleocapsid protein

Carrier: carrier of PLCG2 p.P522R, non-carrier; not a carrier of PLCG2 p.P522R. PBMCs; peripheral blood mononuclear cells, Ig; Immunoglobulin

An additional flowcytometry panel was used to evaluate expression of non-phosphorylated PLCγ2 in various cell populations (**Table S2**). Here, samples were processed according to the bulk lysis protocol for staining of 2.5 x 10^6 cells (www.EuroFlow.org).

For precise enumeration of cells, we used Perfect-Count Microspheres™ (Cytognos) according to the EuroFlow SOP (protocol available on www.EuroFlow.org). In short, 50µl of well-mixed Perfect Count Microspheres were added to 50µl of peripheral blood. This mixture was incubated for 30 min with antibodies directed against CD19, CD3 and CD45. Next, 500µl of NH4Cl was added to lyse the red blood cells. After a 10 min incubation with NH4Cl, samples were immediately acquired on a BD FACS LSR Fortessa 4L, or a BD FACS LSR Fortessa X-20 4L (both BD Biosciences, San Jose, CA, USA).

Measurement of phosphorylated PLCγ2

For in vitro stimulation assays, PB-HEP from Cohort II was used <12h after collection. Intracellular expression of phosphorylated PLCγ2 (pPLCγ2) was measured to assess B-cell activation upon stimulation with IgM or IgG Fabs (being F(ab)2 fragment Goat anti-human IgM Heavy Chain secondary antibody (Southern Biotech), and F(ab)2 fragment Goat anti-human IgG (Jackson ImmunoResearch), respectively). First, PB-HEP was subjected to a bulk lysis to remove red blood cells (protocol at www.EuroFlow.org). Then, cells were incubated with an antibody cocktail for surface staining (45 min, RT in the dark) (**Table S2**), washed with PBS, incubated with 1µl 1:10 Zombie NIR™ Fixable Viability Dye (BioLegend) for 30 min at RT and washed again. Subsequently, cells were resuspended in 230µL PBS+0.5% BSA and incubated with 10µg anti-IgM F(ab)2 or anti-IgG F(ab)2 fragments (10 min at 37°C in a shaking water bath). The reaction was stopped by adding 62.5µl Inside fix (Cell signaling buffer set A; Miltenyi) and incubating for 10 min in the dark. Afterwards, cells were washed and permeabilized (Cell signaling buffer set A, Miltenyi), washed again and resuspended in PBS+0.5% BSA. Next, antibodies to detect pPLCγ2 and immunoglobulins were added (30 min at RT in the dark). After a final washing step, cells were resuspended in PBS and acquired on a BD FACS Canto II 3L. Integrated MFI (iMFI) was calculated according to the following equation (**E1)**:(29)

E1: integrated MFI=% pPLCγ2 positive cells ×MFI pPLCγ2 positive cells

As the stimulated B-cell receptor could not be targeted for antibody stain to identify cells, the following marker combinations were used to identify B-cell subsets: For IgM stimulation: pre-GC B cells, CD20+CD27-IgG-IgA-; unswitched MBCs, CD20+CD27+IgG-IgA-; class-switched MBCs, CD20+CD27+IgG+ or CD20+CD27+IgA+. For IgG stimulation: pre-GC B cells, CD20+CD27-IgD+IgA-; unswitched MBCs, CD20+CD27+IgD+IgA-; class-switched IgG MBCs, CD20+CD27+IgD-IgA-.

Calcium flux assay
Peripheral blood mononuclear cells (PBMCs) from Cohort I and II were isolated from fresh PB-HEP by means of a density gradient (in-house; Ficoll-amidotrizoate, density 1.077g/mL) and stored in liquid nitrogen (freeze medium; RPMI + 40%FCS + 10% DMSO). At the day of analysis, PBMCs were thawed and washed twice with loading buffer (HBSS + 10mM HEPES + 5% FCS). Next, cells (10 x 10^6 PBMCs/mL) were loaded with Indo-1 Calcium Sensor Dye (Fisher Scientific, final concentration 2µg/mL) for 30 min at 37°C, labeled with antibodies directed against cell surface markers and incubated for additional 15 min at 37°C (**Table S2**). Subsequently, cells were washed with 10-20x labeling volume in Flux buffer (HBSS + 10mM HEPES + 5% FCS + 1mM CaCl2) and resuspended in 500µl Flux buffer. Samples were measured immediately on a Cytek Aurora 5L flow cytometer.

After establishing a ~2.5 min baseline, cells were stimulated with 20µL (10 µg) anti-IgM F(ab)2 Fragments (Southern Biotech) or 8.3µl (10 µg) anti-IgG F(ab)2 Fragments (Jackson ImmunoResearch) and measured for ~10 min. Finally, ionomycin was added (5µl, 1mg/mL in DMSO) and samples were measured for ~2.5 minutes. Acquisition was performed at medium speed (~30µl/min). During stimulation and measurement, samples were kept at 37°C in a tube heating device. Indo-Free and Indo-Bound signal was detected in the UV7 and UV1 detector, respectively. Samples were analyzed by dividing the sample into 30 time slots (of equal time, ~30 sec) with the Infinicyt Software (Cytognos) and determining the UV1/UV7 ratios in each time slot. Time slots 1-5 represent baseline signal, time slots 6-25 represent Fab-stimulated signal, and time slots 26-30 represent ionomycin-stimulated signal. MFIs of all time slots were used to plot a curve per B-cell population, from which the area under the curve (AUC) was determined for each individual sample using the GraphPad PRISM Software (v8.1.1). To calculate AUC for the 'total Fab stimulation', time slots 6-25 were used. When calculating the AUC for the 'peak of Fab stimulation', time slots 7-12 were used, as these were the highest values in all donors and presented the peak of calcium release. 'Ionomycin stim' AUC was calculated using time slots 26-30. In all cases, AUC was only calculated for points higher than baseline signal (unstimulated sample). As the stimulated B-cell receptor could not be targeted for antibody stain to identify cells, the following marker combinations were used to identify B-cell subsets: For IgM stimulation: pre-GC B cells, CD20+CD27-IgG-IgA-; unswitched MBCs, CD20+CD27+IgG-IgA-; class-switched MBCs, CD20+CD27+IgG+ or IgA+., and for IgG stimulation: pre-GC B cells, CD20+CD27-IgD+IgA-; unswitched MBCS, CD20+CD27+IgD+IgA-; class-switched IgG MBCs, CD20+CD27+IgD-IgA-.

KREC analysis to determine cell proliferation history
PB-HEP from Cohort II was used <24h after collection for high-speed cell sorting of pre-GC B cells (CD19+CD27-IgM+IgG-IgA-), unswitched MBCs (CD19+CD27+IgM+IgG-IgA-) and class-switched MBCs (CD19+CD27+IgM-IgG+ or CD19+CD27+IgM-IgA+) using a BD FACS Aria III 4L (BD Biosciences, San Jose, CA, USA). On average, a purity of at least 98% was reached for pre-GC B

cells, unswitched MBCs, and class-switched MBCs, respectively. KREC numbers were determined as previously described.(30, 31) In short, DNA of sorted populations and the KREC control cell line (DB01) was isolated with a QIAmp microkit (QIAGEN) and DNA concentrations were determined by NanoDrop 2000 (Thermo Fisher Scientific). Next, we performed qPCR (Quantstudio qPCR Machine, Thermo Fisher Scientific) to quantify the average amount of coding joints (Cj), signal joints (Sj) and Albumin (Alb) in each B-cell population and the control cell line (DB01), using the primers that were previously described by van Zelm and colleagues.(30) The number of cell divisions (ΔCt) for each B-cell population was calculated with the following equation (**E2**):

E2: $\Delta Ct = Ct(Sj) - Ct(cj) - \Delta Ct(control)$

Where ΔCt (control) is a standard correction for primer efficacy based on the Ct(sj) and Ct(Cj) from DNA from the DB01 control cell line.

Phagocytosis of pHRodo™ Green *E. coli* Bioparticles

Assessment of the phagocytic capacity was performed with opsonized *E. coli* (pHRodo™ Green *E. coli* Bioparticles, ThermoFisher). Polystyrene FACS tubes (4mL) were filled with 200µl PB-HEP (Cohort II, <12h after collection) and placed on ice for at least 10 minutes. Then, 40µl of pHRodo™ Green *E. coli* was added, samples were mixed and incubated at 37°C for exactly 20 min. All further steps were performed on ice or at 4°C to stop the reaction. Cells were washed and stained (30 min on ice in the dark) with an antibody cocktail (**Table S2**). Next, samples were lysed with BD lyse (10 min, rolling at 4°C). Lastly, cells were washed, resuspended in cold PBS with 0.5% BSA and acquired at a Cytek Aurora 3L flow cytometer. To prevent shedding of CD62L, TAPI-2 (final concentration of 20µM) was always present. To account for background activation or signal, several control tubes were measured in addition to the sample tubes (**Table S3**).

Production of reactive oxygen species (ROS)

Production of ROS upon stimulation was assessed with the phagoBURST kit (PHAGOBURSTTM CE/IVD kit, BD Biosciences) according to manufacturer's protocol with some modifications, as described further in this paragraph. In short, each tube was filled with 200µl PB-HEP (Cohort II, <12h after collection) and placed on ice for at least 10 minutes. Then, 20µl of wash buffer (reagent A), Phorbol 12-Myristate 13-acetate (PMA) (Sigma, P8139-1mg, final concentration 600ng/mL), or *E. coli* (reagent B, well-mixed by pipetting) was added to each tube. After proper mixing, tubes were incubated for exactly 10 min at 37°C in a shaking water bath. Next, 20µl of substrate (dihydrorhodamine -DHR123, reagent E) was added to each tube and mixed. Tubes were incubated for another 10 min at 37°C. Subsequently, the assay was stopped by lysing the cells (reagent F, 15 min, RT, dark). Cells were washed twice, stained for 15 min in the dark at RT with antibody cocktail (Table S2) and PBS with 0.5% BSA, washed again, resuspended in PBS with 0.5% BSA and stored on ice until acquisition on a Cytek Aurora 3L flow cytometer (<1h). To prevent shedding of CD62L, TAPI-2 (final

concentration of 20μM) was always present. The rhodamine 123 (R123) signal was used as a readout for ROS production (conversion from DHR123 to R123). To account for background activation or signal, several control tubes were measured in addition to the sample tubes (**Table S4)**.

Data integration phagocytosis and ROS production

The phagocytosis assay and the ROS production were considered complementary assays in which we evaluated three aspects of phagocytosis. First, we evaluated the percentage of phagocytosing cells, then we combined this – together with the pHRodo™ Green signal- into the integrated MFI (iMFI)(29), which was used as a measure of how many particles each cell has phagocytosed (**E3**). For ease of interpretation, this value was divided by 100,000.

E3: integrated MFI=% E.coli positive cells ×MFI E.coli positive cells

Lastly, we measured the production of ROS upon phagocytosis and combined this with the iMFI into one output; the normalized ROS production, which was defined as the ROS generation per given number of phagocytosed particles (**E4**).

E4: normalized ROS production= (R123 MFI)/(integrated MFI)

***In vivo* evaluation**

We collected additional blood samples from donors (Cohort III), 7-14 weeks after their second vaccination against SARS-CoV-2. Serum antibodies directed against the Spike (S) protein, Receptor Binding Domain (RBD) and Nucleocapsid (N) protein were determined by a fluorescent-bead-based multiplex immunoassay (MIA), as previously described.(32) In short, the stabilized pre-fusion conformation of the ectodomain of the Spike protein, the receptor binding domain of the S-protein (RBD) and the Nucleocapsid (N) protein were each coupled to beads or microspheres with distinct fluorescence excitation and emission spectra. Serum samples were diluted and incubated with the antigen-coupled microspheres. Following incubation, the microspheres were washed and incubated with phycoerythrin-conjugated goat anti-human, IgG, IgA, and IgM. The data were acquired on the Luminex FlexMap3D System and MFI was converted to international units per milliliter (IU/ml), using Bioplex Manager 6.2 (Bio-Rad Laboratories) software.

Data analysis and statistical analysis

Flow cytometry data was analyzed with Infinicyt software (version 2.0.3.a. and 2.0.4.b., Cytognos, Spain). Statistical analysis was performed in GraphPad Prism 8.1.1 software (GraphPad, San Diego, CA, USA). Differences between p.P522R carriers and non-carriers, were evaluated using the Mann-Whitney test. Impact of age was assessed using Spearman's correlation. $P<0.05$ was considered significant.

Results

Numbers of circulating immune cells in the study cohort are representative for healthy aged adults

Upon aging, the composition of the immune system changes. The median age of the studied cohort was 72 years (range: 59 -103 years), as most of the donors were children of a centenarian who carried the p.P522R variant, and only a few were centenarians or siblings from a centenarian (details provided in **Methods section** and **Table 1**). To assess to what extent this cohort represented the general (age-matched) population, we first compared absolute counts of multiple innate and adaptive cell populations with reference values from healthy age-matched cohorts.(24, 26, 27) (ref 22: van der Pan et al, manuscript in revision) Overall, innate, CD4 T- and B-cell counts in the donors were representative of their age category, with exception of IgG3, IgG4 and IgA2 plasma cells, which were slightly elevated in several donors. In three donors (carriers, one family), a subclinical B-cell expansion was observed. Additionally, two donors (non-carriers, different families) in whom we observed B-cell aberrancies were excluded from all further analyses and referred to a hemato-oncologist for further evaluations (the expanded B-cell phenotypes observed in the initial research-based screening were: CD19+CD20+CD5+CD21+CD27+IgM+IgD-/dim and CD19+CD20+CD5+CD21dimCD27+IgG1dim). For CD8 T- and NK-cell subsets no age-matched reference values were available. No impact of sex on cell counts was observed. An impact of age on cell counts was found for several subpopulations. To reduce impact of sex or age on the comparison between p.P522R carriers and non-carriers, cohorts were sex- and age-matched as much as possible. Lastly, we observed a pronounced effect of pedigree, as in several subsets cell counts from all first-degree family members tended to cluster together, even when individuals were living at different locations for many years (**Figure S1**).

Several parameters in p.P522R carriers resemble younger healthy donors

To evaluate the impact of PLCγ2 carriership on cell counts in innate and adaptive immune cell subsets, we related this information to the carriership status. Overall, p.P522R carriers tended to have higher total and immature B-cell numbers, and significantly more CD20++CD21-CD24+ naive and IgG1+ MBCs (**Figure 1A**). This pattern was observed in at least half of the families with mixed carriership (CD20++CD21-CD24+ naive B cells; 3/6, IgG1+ MBCs; 5/6 families). Interestingly, upon comparing median cell counts carriers and non-carriers with an internal reference cohort (n=25, 9 females, aged 18-54, median age: 27 years), the carrier cell counts more closely resembled the counts of the younger cohort than the non-carriers (**Figure 1A**). Interestingly, for the CD20++CD21-CD24+ naive B cells, the median cell count was slightly higher in carriers than in the younger cohort.

Next, we evaluated expression of several surface markers: HLA-DR, CD62L, CD16, CD33 and FcεRI on innate immune cells, CD45RA, CD27, CD28 and CD3 on T cells, and CD20 and CD21 on B cells. Interestingly, we found a reduced ex-

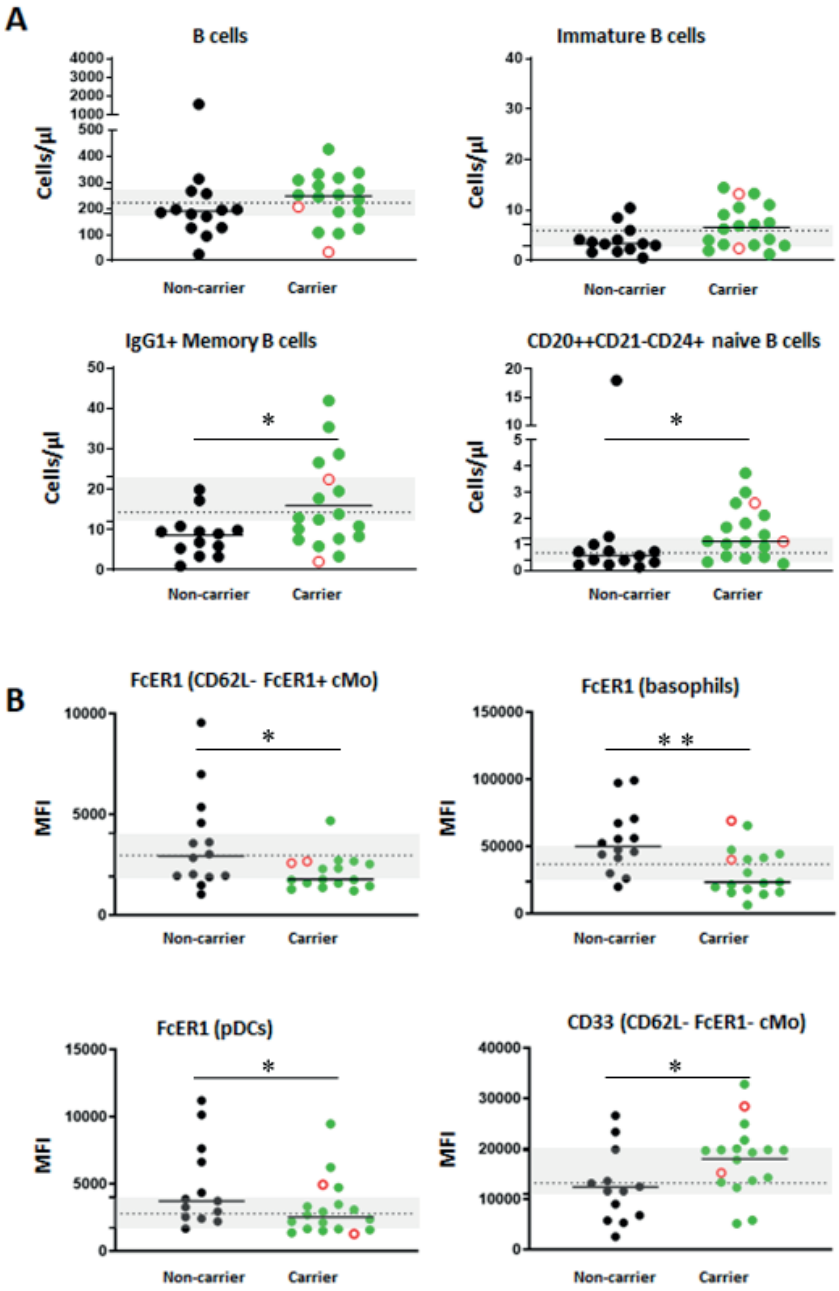

Figure 1. Main differences between PLCγ2 p.P522R carriers and non-carriers in Cohort I. (A) Major differences in absolute immune cell counts between carriers and non-carriers. (B) Major differences in activation marker expression between carriers and non-carriers. Mean fluorescence intensity (MFI) was corrected by subtraction of background signal on a negative reference population. Differences between cohorts were determined using the Mann-Whitney test. Green circles indicate p.P522R carriers, and black circles indicate non-carriers. Centenarian data points are indicated in the graphs as an open red circle. Grey boxes indicate the 95%CI and dashed lines indicate the median cell count or MFI from a younger reference cohort (n=25, average age: 31 years old), whose data was collected in the same laboratory, using identical methods and equipment. N=31, * $p<0.05$, ** $p<0.01$.

pression of FcεRI on CD62L- FcεRI+ classical monocytes (CD62L- FcεRI+ cMo), basophils and plasmacytoid dendritic cells (pDCs) in p.P522R carriers with a median age of 71 years (range 59-103 years) versus non-carriers with a median age of 74 years (range 61-83 years) (Figure 1B). Median FcεRI expression in carriers was below, or in the lower range, of the young reference cohort (n.s.). In contrast to FcεRI expression, the expression of CD33 on CD62L- FcεRI- cMos was increased in the p.P522R carriers, and in the high range of the 95% confidence interval of the younger reference cohort, while non-carriers resided on the lower end of the 95% confidence interval of the younger reference cohort (n.s.) (**Figure 1B**).
Higher PLCγ2 expression in immune cells of p.P522R carriers

Then, we evaluated the PLCγ2 expression levels in different leukocyte populations in the total cohort (irrespective of carriership). The highest PLCγ2 expression was found in eosinophils, with high variation between individuals, and, more consistently, in antigen-experienced B cells (**Figure 2A**). When comparing carriers with non-carriers, the levels of PLCγ2 in all evaluated B-cell subsets were consistently higher in p.P522R carriers than in non-carriers (**Figure 2BC**). Likewise, innate cells tended to have slightly higher median values for PLCγ2 expression in p.P522R carriers compared to non-carriers (**Figure 2BC**).

To summarize our findings in this first analysis (e.g. Cohort I): based on cell counts, Cohort I seemed representative for healthy individuals of this age group. Whenever differences in cell counts were found between p.P522R carriers and non-carriers, carriers more closely resembled the younger control cohort. Lastly, PLCγ2 expression tended to be higher in carriers, mostly on antigen-experienced B cells.

Higher levels of phosphorylated PLCγ2 in stimulated B cells from p.P522R carriers

In a second analysis (Cohort II), we evaluated the effect of p.P522R on PLCγ2 activity in several B-cell subsets derived from 14 healthy older adults (6 non-carriers, 8 carriers) (**Table 1, Text S1**). As PLCγ2 is located downstream of the BCR, we assessed whether specific elements of the signaling pathway were affected by the carriership status. The BCR was stimulated with IgM (stimulation with IgG Fabs was also tested, but results were considered unreliable due to high background signal). In the steady state, we observed no significant difference between the levels of phosphorylated PLCγ2 (pPLCγ2) in B cells from p.P522R carriers and non-carriers (Figure 3A). Upon BCR stimulation with IgM Fabs, a similar percentage of unswitched MBCs was activated, but the integrated mean fluorescent intensity (iMFI) of PLCγ2 was almost two-fold higher in carriers than in non-carriers (3667 vs 2051, respectively), implying a stronger activation in carriers (**Figure 3A**). Moreover, levels of pPLCγ2 tended to be higher in stimulated pre-GC B cells in carriers. According to expectations, no increase in pPLCγ2 was observed upon IgM stimulation in the (IgM-) class-switched MBCs in either group.

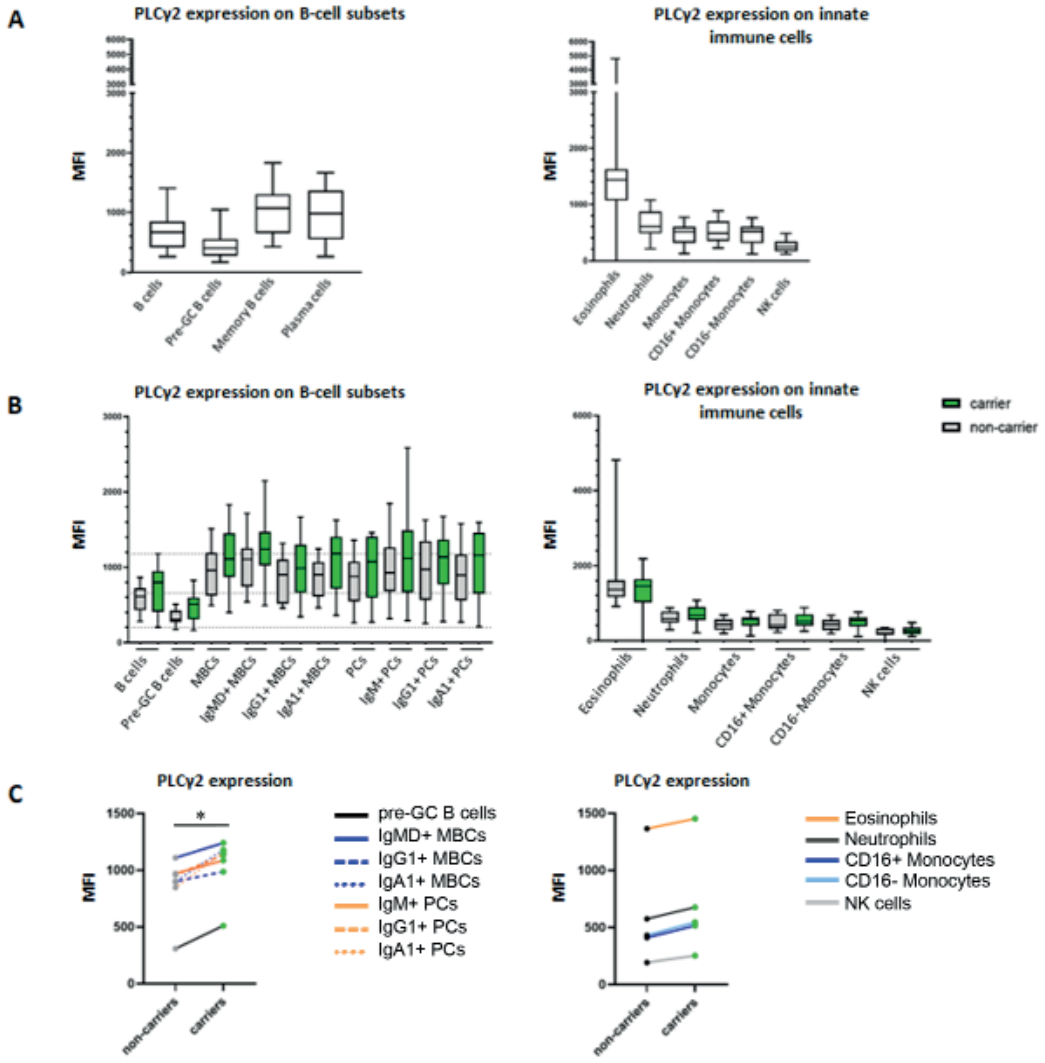

Figure 2. PLCγ2 expression in different populations of circulating immune cells. (A) PLCγ2 expression measured as mean fluorescence intensity (MFI) and corrected for background signal by subtracting the MFI signal of a negative reference population (T cells) of the total cohort (irrespective of p.P522R carriership). N= 31. (B) PLCγ2 expression on B-cell and myeloid cell subsets in p.P522R carriers (green) and non-carriers (grey). Dashed lines represent the median (min-max) of PLCγ2 expression of B cells of the total cohort. (C) PLCγ2 expression on B-cell and myeloid cell subsets between carriers (green) and non-carriers (grey). The median of each subset is plotted, medians of the same subset are connected with lines. Differences were evaluated with Mann-Whitney test. MBC; memory B cell, IgMD+ MBC; unswitched memory B cell, Pre-GC; pre-Germinal Center B cells, PC; plasma cells, NK cells; Natural Killer cells. * $p<0.05$.

Higher calcium flux in B cells upon BCR stimulation in p.P522R carriers

Next, we evaluated the effect of p.P522R further downstream of the BCR by measuring the calcium release ('calcium flux') upon BCR stimulation using IgM Fabs. After a pilot experiment using IgM and IgG Fab stimulation in 12 donors, we found IgM stimulation to be most robust (**Figure S2**). We observed no differences in calcium flux in pre-GC B cells derived from Cohort II donors (**Figure 3B**), but there was a trend towards more robust calcium flux in p.P522R carriers vs non-carriers upon Fab stimulation in unswitched MBCs ('Total flux' and 'Flux at peak') (**Figure 3C**). However, this trend was not observed when comparing the calcium flux of all donors included in cohort I and II (**Figure S3**). Again, stimulation with IgM Fabs did not result in calcium release in class-switched MBCs, thus confirming that the measured calcium flux is truly due to BCR-specific stimulation (**Figure 3D**).

No difference in number of cell divisions between carriers and non-carriers

Stronger B-cell activation upon stimulation in p.P522R carriers may result in more robust proliferation upon antigen encounter. To test this hypothesis, we evaluated B-cell replication history with the KREC (kappa-recombination excision circle) assay. Despite generally low cell counts, we were able to determine that pre-GC B cells measured in all 14 individuals in Cohort II had undergone on average 1.58 cell divisions, while unswitched MBCs measured in 8/14 individuals, had undergone on average 7.82 cell divisions (**Figure 3E**). These findings are in line with previous publications.(31) We observed no clear difference in replication history of B-cell subsets between p.P522R carriers and non-carriers, possibly due to the limited number of donors in the non-carrier cohort (replication history in pre-GC B cells: 1.43 vs 1.64; in unswitched MBCs: 7.12 vs 7.82 (**Figure 3F**)). Lastly, although class-switched MBC samples were collected as well, the obtained cell numbers were generally too low to determine the number of undergone cell divisions.

Serum Ig responses to SARS-CoV-2 vaccination comparable between p.P522R carriers and non-carriers

To test whether the effect of p.P522R on B-cell activation as observed in our *in vitro* experiments also translates to an *in vivo* effect (e.g. effect on antibody production), we recognized a window of opportunity in the current global vaccination efforts against SARS-CoV-2. We collected serum samples from 22 individuals (Cohort III), 7-14 weeks after receiving a second vaccination against SARS-CoV-2. Donors were vaccinated with Comirnaty® (Pfizer/BioNTech, 9 carriers, 9 non-carriers); Spikevax® (Moderna, 1 carrier); Vaxzevria® (AstraZeneca, 1 non-carrier), or did not indicate vaccine type (2 non-carriers). All donors developed prominent IgG responses against the viral Receptor Binding Domain (RBD) and Spike (S)-protein. Antibody responses against the viral Nucleocapsid (N)-protein – indicative of viral infection- were predominantly IgM responses (**Figure 4A, B**). No differences were observed between p.P522R car-

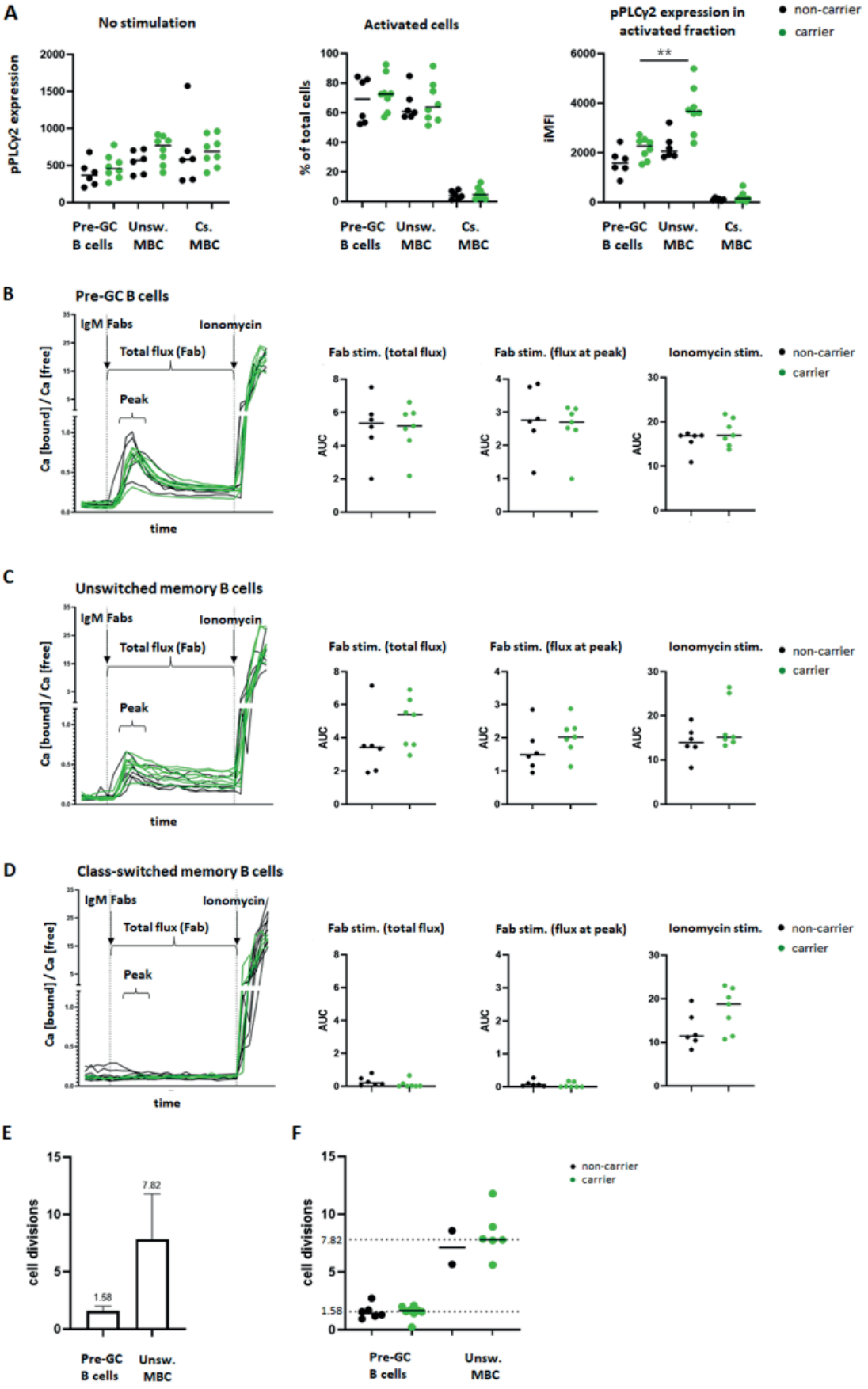
A
No stimulation
Activated cells
pPLCγ2 expression in activated fraction
pPLCy2 expression
% of total cells
iMFI
**
Pre-GC B cells
Unsw. MBC
Cs. MBC
non-carrier
carrier
B
Pre-GC B cells
IgM Fabs
Ionomycin
Total flux (Fab)
Peak
Ca [bound] / Ca [free]
time
Fab stim. (total flux)
Fab stim. (flux at peak)
Ionomycin stim.
AUC
C
Unswitched memory B cells
D
Class-switched memory B cells
E
cell divisions
7.82
1.58
F

Figure 3 (previous page). Assessment of B-cell activation upon IgM Fab stimulation and B-cell replication history in p.P522R carriers and non-carriers. (A) Expression of phosphorylated PLCγ2 (pPLCγ2) in B cells before and after stimulation of the B-cell receptor with IgM Fabs. Detection of pPLCγ2 was used as a direct measure of B-cell receptor activation after IgM Fab stimulation. N=14. (B-D) Measurement of calcium release ('flux') after B-cell stimulation with IgM Fabs of pre-GC B cells (CD27-IgG-IgA-) (B), unswitched memory B cells (CD27+IgG-IgA-) (C), or class-switched memory B cells (CD27+IgG+ or CD27+IgA+) (D) in cohort II. Differences between carriers and non-carriers were evaluated by comparing the area under the curve (AUC) of the total Fab stimulation (from stimulation until the moment ionomycin was added, ~ 10 min, flux intensity and duration), the peak of the response after Fab stimulation (the 5 highest points after the Fabs were added to the cells; flux intensity), and after ionomycin was added (to determine the maximum flux). AUC was calculated only for points that were higher than baseline value (unstimulated sample). N=13 (one sample was lost due to technical failure). (E+F) Measurement of the average number of undergone cell divisions by total pre-GC B cells (CD27-IgM+IgG-IgA-) or unswitched memory B cells (CD27+IgM+IgG-IgA-) by means of qPCR based KREC assay in the total cohort (E) or separated into carriers and non-carriers (F). For pre-GC B cells; n=14. Due to low DNA concentration, for unswitched MBC; n=8. Differences were evaluated by Mann-Whitney test. Pre-GC; pre-Germinal Center, MBC; memory B cells, iMFI; integrated mean fluorescence intensity (for calculation, see Methods) Unsw. MBC; unswitched memory B cells, Cs. MBC; class-switched memory B cells. ** p<0.01.

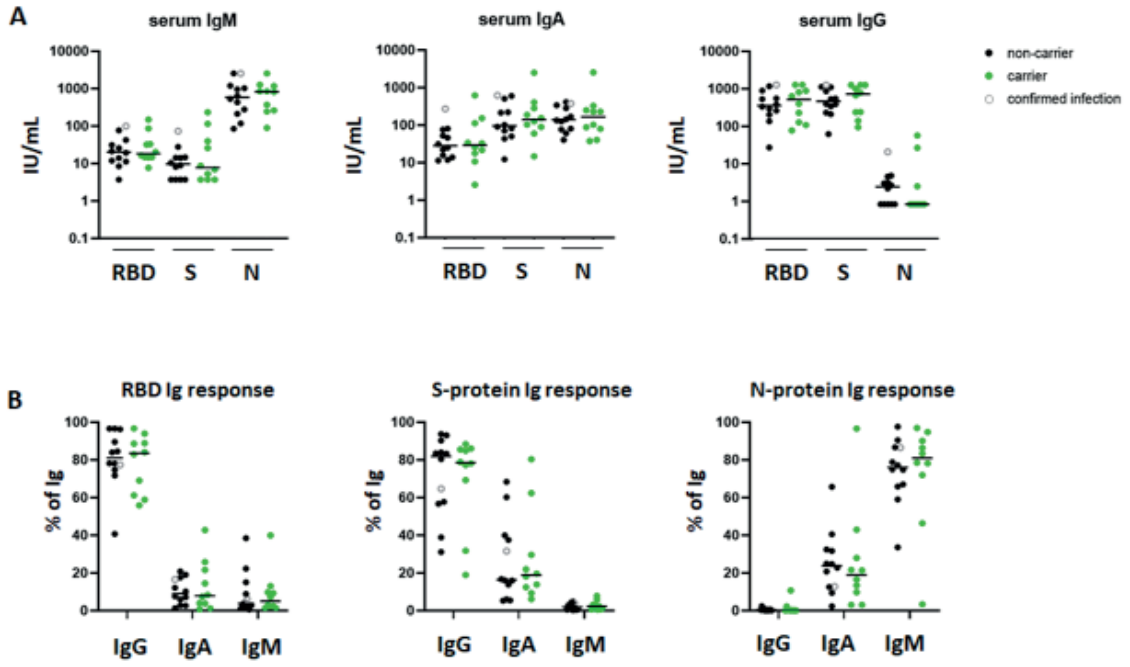

Figure 4. Response to SARS-CoV-2 vaccination in p.P522R carriers and non-carriers. Samples were donated 7-14 weeks after second vaccination. Type of vaccine received by donors: Comirnaty® (Pfizer/BioNTech) – 9 carriers, 9 non-carriers; Spikevax® (Moderna)- 1 carrier, 0 non-carriers; Vaxzevria® (AstraZeneca) – 0 carriers, 1 non-carrier; vaccine type not indicated- 0 carriers, 2 non-carriers. One donor reported a confirmed SARS-CoV-2 infection, this donor is indicated with an open grey circle. (A) Serum IgM, IgA, and IgG response against the receptor binding domain (RBD), spike protein (S-protein) and nucleocapsid protein (N-protein), expressed in IU/mL. (B) Composition of the serum Ig response per antigen, expressed as % of total antigen-specific Ig response.

riers and non-carriers.

Summarizing our (B-cell related) findings in Cohort II/III: PLCγ2 in unswitched MBCs from p.P522R carriers is more strongly phosphorylated upon stimulation compared to non-carriers. Moreover, the calcium flux in p.P522R carriers was increased relative to non-carriers, at least in individuals from Cohort II, who were selected based on fewer comorbidities. Due to technical limitations, we were unable to obtain reliable results for class-switched memory cells, such that it is currently unclear to what extent these data can be extrapolated to other MBC subsets. Despite clear differences between p.P522R carriers and non-carriers in the multiple *in vitro* functional experiments, *in vivo* antibody responses raised against SARS-CoV-2 vaccine were comparable between carriers and non-carriers.

Increased ROS production upon FcR-mediated stimulation of innate immune cells in p.P522R carriers

Besides being located downstream of the BCR, PLCγ2 is also located downstream of FcRs, which are present on many cells of the innate immune system, including the microglia of the brain. Therefore, we evaluated ROS production and phagocytic activity upon FcR-mediated stimulation in several cell types of the innate immune system: neutrophils, classical, intermediate, and non-classical monocytes (cMos, iMos and ncMos, and their subsets), and myeloid and plasmacytoid dendritic cells (mDCs, pDCs, and their subsets).

Although the percentage of phagocytosing cells did not differ between p.P522R carriers and non-carriers (**Figure 5A**), the iMFI, reflecting the amount of phagocytosed *E. coli* particles per cell (phagocytic capacity), tended to be lower in carriers. This trend was especially prominent in classical and non-classical monocyte subsets, less prominent in CD14- mDC subsets and iMos, and not observed in CD14dim mDCs (**Figure 5A, Figure S4**).

In addition to phagocytosis, we evaluated ROS production upon phagocytosis of opsonized *E. coli* particles (PhagoBURST assay). No difference between p.P522R carriers and non-carriers was observed in the amount of ROS produced (**Figure 5A, Figure S4**). To combine information from both assays, we investigated ROS production relative to the number of phagocytosed particles. We observed that this 'normalized ROS production' was increased in carriers, which was especially evident in CD62L-cMos (**Figure 5A**). Also, we observed that the ROS production relative to number of phagocytosed particles tended to be increased (n.s.) in carriers across all evaluated monocyte subsets and neutrophils (**Figure 5B, Figure S4A-C**). Lastly, we observed increased normalized ROS production in CD14- mDCs, but not in CD14dim mDCs (**Figure S4D-E**). Thus, the ROS generation per particle tends to be somewhat higher in several cell populations in p.P522R carriers compared to non-carriers.

Additionally, we stimulated samples with Phorbol 12-Myristate 13-acetate (PMA), which results in FcR-independent ROS generation. Surprisingly, we observed

a trend towards decreased ROS production in p.P522R carriers compared to non-carriers, which was seen for neutrophils, monocyte subsets and DC subsets (**Figure S5**). This effect was the strongest in monocytes, especially in CD62L+ and CD62L- cMos, where p.P522R carriers showed a significantly lowered ROS production compared to non-carriers.

Thus, upon stimulation with opsonized *E. coli*, we observed that p.P522R carriers had a lower phagocytic capacity despite overall similar ROS production upon phagocytosis of *E. coli* and thus had increased ROS production relative to the number of opsonized particles. Nevertheless, the total FcR-independent ROS generation was lower in these same carriers. In general, differences were most prominent in the monocyte subpopulations.

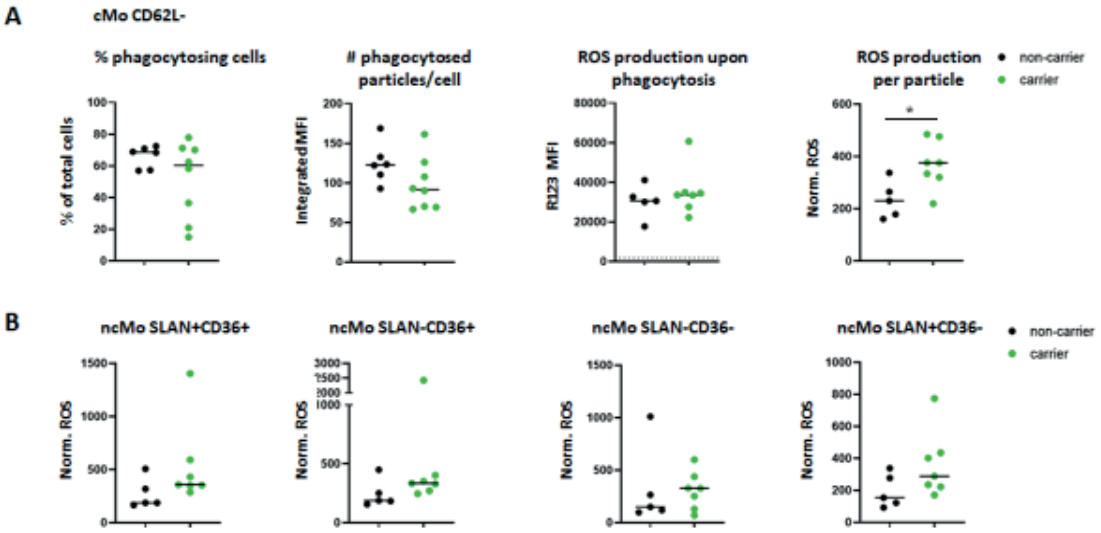

Figure 5. Detection of phagocytosis and ROS production in monocyte subsets after stimulation with pHRodo™ Green *E. coli* bioparticles. (A) To evaluate the outcome of the phagocytosis assays, three different readouts were used per population; % of cells that were phagocytosing, the average amount of particles phagocytosed per cell, and the ROS production upon phagocytosis (as measured by conversion of DHR123 into R123). The average amount of particles phagocytosed per cell and the ROS production were further combined into one value; the ROS produced per particle, or the 'normalized ROS' (calculations are indicated in the Methods). The values are presented for the CD62L- classical monocyte (cMo) subset (B) The normalized ROS of all four defined non-classical monocyte (ncMo) subsets, based on expression of CD36 and SLAN. Differences were evaluated by means of Mann-Whitney test. All readouts were corrected for background/baseline activation by subtracting the value of the control (ice) from the activated (37°C) sample. * $p<0.05$.

Discussion

In this study, we investigated the impact of PLCγ2 variant p.P522R on the immune system in older adults. We showed that p.P522R carriers had higher numbers of circulating CD20++CD21-CD24+ naive B cells and IgG1+ MBCs, lower expression of FcεRI on several innate immune cells (pDCs, basophils and CD62L-

FcεRI+ cMos), and higher expression of CD33 on CD62L- FcεRI- cMos. Overall PLCγ2 expression tended to be higher in p.P522R carriers. Upon BCR stimulation, the levels of phosphorylated PLCγ2 were significantly higher in unswitched MBCs derived from in p.P522R carriers compared to non-carriers, and we observed a trend towards higher calcium flux. This suggests that B-cell stimulation in p.P522R carriers leads to a stronger activation compared to non-carriers. The number of cell divisions undergone by pre-GC B cells and unswitched MBCs was not different between p.P522R carriers and non-carriers. Upon vaccination against SARS-CoV-2, vaccine-specific antibody levels did not differ between p.P522R carriers and non-carriers. We also evaluated phagocytosis and ROS production in myeloid cells and found the most prominent differences in the monocyte subsets, where upon FcR-dependent stimulation, (normalized) ROS production was increased in carriers. In contrast, FcR-independent ROS generation was lowered in these same carriers. Across all experiments, the observed effects are small, which is in full accordance with our expectations: the molecular interplay that makes up a robust immune system function has evolved under high evolutionary pressure, such that only subtle changes will be tolerated to have an advantageous effect.

To our knowledge, this is the first study that investigates the effect of the PLCγ2 variant p.P522R in the human immune system ex-vivo and in-vivo. Previous studies have reported that -amongst others- the genetic constellation, unique to all individuals, has a profound influence on cell counts.(33, 34) In line with these previous studies, we observed an effect of pedigree on the numbers of circulating immune cells. Using human subjects means accepting to sample in individuals from a heterogenous genetic background compared to inbred animals or cell lines. To minimize genetic heterogeneity, we set out to select samples of p.P522R carrier and non-carrier siblings. These siblings (~71/72-year-old) were children from a parent who participated in the 100-plus Study, who reached at least 100 years and carried the protective p.522R PLCγ2 variant.(20) We acknowledge that, next to the protective variant in PLCγ2, these individuals, both p.P522R carrier and non-carrier siblings, may be enriched with additional advantageous genetic elements associated with prolonged health which may positively affect immune system function. Nevertheless, comparison with age-matched reference cohorts confirmed that cell counts were representative for the general older adult population.

Upon BCR-stimulation, B cells in p.P522R carriers showed a stronger activation. This was most prominent for unswitched MBCs. Due to technical limitations, we were unable to confirm whether the same holds true for class-switched MBCs. In vitro studies that investigated the activation levels of unswitched and class-switched MBCs reported conflicting data, and thus indicate that future studies are required.(35) Nonetheless, the in vitro stimulation of B cells from the homogenous and healthy individuals in Cohort II suggested that the activation signal in carriers was stronger, which is in line with the suggestion that the p.P522R variant is a functional hypermorph, as previously observed in cell lines and mouse models.

(13, 18, 19) However, this pattern was lost upon the combination of Cohort II with Cohort I. Cohort I was a more heterogenous cohort including individuals with diverse comorbidities or medication use that may influence the immune responses, such as (undiagnosed) autoimmune disease, use of steroids, or use of non-steroid anti-inflammatory drugs (NSAIDs).

While our analysis of post-vaccination serum responses did not reveal a beneficial effect of p.P522R in terms of generated serum levels of IgG, IgM or IgA, the complexity of the generated response (e.g., B-cell repertoire) may differ between p.P522R carriers and non-carriers. Previous studies indicated that with increasing age the diversity of the B-cell repertoire decreases(36, 37), therefore, an in-depth evaluation of the Ag-specific B-cell repertoire, especially their VDJ regions, may reveal differences between p.P522R carriers and non-carriers. Although we did not investigate repertoire in this study, the higher numbers of circulating CD20++CD21-CD24+ naive B cells in carriers may represent a broader available B-cell repertoire. This may leave carriers better equipped to deal with neoantigens.

Innate immune cells in p.P522R carriers had a lower expression of FcεRI which, upon activation, contributes to the production of important immune mediators that promote inflammation (cytokines, interleukins, leukotrienes, and prostaglandins).(38, 39) Allergy-related expression of IgE associates with an upregulation of FcεRI expression(40), but since 5/7 reported allergies were in p.P522R carriers the frequency of a reported allergy could not explain the decreased FcεRI expression among carriers.

While the current study was ongoing, two studies were published that evaluated the impact of p.P55R on phagocytosis. Takalo et al reported increased phagocytic activity of opsonized E. coli (as determined by pHRodo™ Green signal and percentage of phagocytosing cells) in murine p.P522R microglia-like cells (BV2 cell-line) and knock-in murine macrophages.(13) In functional analyses between, macrophages derived from homozygous knock-in mice and wild type littermates, Takalo et al revealed that the p.P522R variant potentiates the primary function of PLCγ2 as a PIP2-metabolizing enzyme.(13) This was associated with improved survival and increased acute inflammatory responses of the knock-in macrophages. Maguire et al showed that -although P522R showed hypermorphic activity in Ca-release and endocytosis experiments-, phagocytosis of opsonized E. coli was reduced in mouse microglia and macrophages and in human iPSC-derived microglia. However, they indicated that reduction of phagocytosis may have been due to substrate deprivation (PIP2) upon prolonged stimulation.(19) The discrepancies between the study of Takalo and Maguire might be explained by differences in experimental setup, such as in the timeframe used for phagocytosis, the type of evaluated readout, concentration of substrate, and the cell types evaluated.

In our study of primary human cells, the number of phagocytosed particles per

cell seemed somewhat reduced in p.P522R carriers, which aligns with our observation that innate immune cells in p.P522R carriers had a higher expression of CD33 which, upon stimulation by any molecule with sialic acid residues (such as glycoproteins or glycolipids), results in a cascade that inhibits phagocytosis in the cell.(41) Importantly, previous studies suggested an association between CD33 levels and the etiology and pathology of Alzheimers' disease: the common CD33 risk allele (rs3865444, associated with increased chance of developing Alzheimers' disease in GWAS) was associated with higher CD33 expression too.(41, 42) However, carriers of the risk allele had a 7-fold increased expression of CD33 on peripheral monocytes.(42) In our study we see a much lower increase in CD33 surface expression in one particular monocyte subset (~1.67-fold, CD62L- FcεRI- cMo). Additionally, our results indicated that the ROS production per phagocytosed particle seemed increased in p.P522R carriers, although overall ROS production between carriers and non-carriers was similar. These findings suggest that p.P522R carriers have a more efficient ROS production per particle. This more efficient ROS production (per particle) may contribute to an increased resilience to age-related decline of immune function as previous studies indicated that with increasing age, both the phagocytic capacity (# particles ingested/neutrophil) and oxidative burst are reduced.(5, 43, 44) The higher ROS production per phagocytosed particle might translate to increased degradation capacity -and thus more effective clearance- within the phagocyte. This capacity has been reported to be decreased in aged individuals as well as Alzheimers' disease patients.(45) While we cannot exclude that other advantageous (genetic) elements carried by these donors also contribute to this phenotype, this more efficient ROS production in p.P522R carriers may protect these individuals from infection and can thus contribute to a long-term maintenance of healthy immune function.

PLCγ2 is not the only molecule expressed on peripheral immune cells that has been shown to associate with protection against neurodegenerative diseases. A recent preprint suggested an association between HLA-variant DRBI*04 and protection against neurodegenerative diseases (HLA-DR is mainly expressed on antigen-presenting cells).(46) In this study we cannot answer the question whether the protective effect of the p.P522R variant on neurodegenerative diseases is translated, perhaps in part, through the peripheral immune system. However, a recent study by Prongpreecha et al suggested that reduced activation of PLCγ2 in PMBCs is a molecular characteristic of Alzheimers' disease.(47) Our findings clearly indicate that both adaptive and innate circulating human primary cells of the peripheral system are subtly changed in carriers of the p.P522R variant. The more efficient ROS production we observed upon FcR-mediated stimulation in peripheral monocytes may translate directly to the microglia in the in vivo human brain, which also express FcR. Therefore, the p.P522R variant may protect the brain with a mechanism similar to that observed in peripheral immune cells. Although there is discussion on whether phagocytosis is beneficial or detrimental during Alzheimers' disease (19, 48), a more efficient clearance of tissue damage and debris in the brain may be beneficial at least in the initial stages of Alzheimers' disease. To what extent a more sensitive B-cell response has

a protective effect on the brain remains to be investigated. However, (natural) antibodies against brain amyloid or tau have been observed not only in Alzheimers' disease patients, but also in cognitively healthy elderly individuals.(49, 50) In fact, in brain proteinopathies, antibodies can enter the brain parenchyma and effectively remove the aberrant proteins, making these antibodies promising candidates for intervention strategies for several types of dementia.(51-53) We may thus speculate that a sensitive B-cell system, such as observed in the p.P522R carriers, through increased activity in the periphery, may contribute to the long-term maintenance of brain health.

Conclusions

Our study confirmed the hypermorphic activity of PLCγ2 p.P522R in circulating immune cells, which provides a low-invasive source of primary cells for future studies. It would be interesting to evaluate whether p.P522R benefits carriers early in life, or whether its protective effect plays a role mostly later in life by, for example, delaying immunosenescence, both in the soma and in the central nervous system. More insight in the functioning of p.P522R may help design future therapies and better define the therapeutic window of PLCγ2.

List of abbreviations

Phospholipase C gamma 2 (PLCγ2)
B and T-cell receptor (BCR, TCR)
germinal center (GC)
memory B-cell (MBC)
reactive oxygen species (ROS)
single-nucleotide polymorphism (SNP)
Phospholipase C gamma 2 gene (PLCG2)
phosphatidylinositol 4,5-bisphosphate (PIP2)
inositol 1,4,5-triphosphate (IP3)
diacylglycerol (DAG)
Fc receptors (FcR)
Triggering Receptors Expressed on Myeloid cells (TREM)
peripheral blood (PB)
Genome Screening Array (GSA)
quality control (QC)
Setup and Tracking beads (CS&T beads)
Dendritic cell-monocyte (DC-monocyte)
CD4-T cell panel (CD4T)
CD8 cytotoxic T-cell panel (CYTOX)
B-cell and plasma cell panel (BIGH)
Peripheral blood mononuclear cells (PBMCs)
area under the curve (AUC)
coding joints (Cj)
signal joints (Sj)
Albumin (Alb)
dihydrorhodamine (DHR123)

classical, intermediate, and non-classical monocytes (cMos, iMos and ncMos)
phosphorylated PLCγ2 (pPLCγ2)
integrated mean fluorescent intensity (iMFI)
kappa-recombination excision circle (KREC)
Receptor Binding Domain (RBD)
Spike protein (S protein)
Nucleocapsid protein (N protein)
myeloid and plasmacytoid dendritic cells (mDCs, pDCs)
Phorbol 12-Myristate 13-acetate (PMA)
non-steroid anti-inflammatory drugs (NSAIDs)

Declarations
Ethics approval and consent to participate: In this study, we selected 36 individuals from the 100 plus study cohort, as previously described by Holstege et al (METC number: 2016.440, approved by the Medical Ethics Committee of the VU University Medical Center, Amsterdam, the Netherlands). Informed consent was obtained from each study participant.

Consent for publication: not applicable.

Availability of data and materials: The datasets used and/or analysed during the current study are available from the corresponding authors on reasonable request. Questions and requests about the clinical data should be submitted to H. Holstege. Questions and requests for the experimental data discussed in this manuscript should be submitted to J.J.M. van Dongen.

Funding/Competing interests: This work was supported by the HorstingStuit Foundation, the Hans und Ilse Breuer Foundation and Stichting VUmc Fund; and by the ABOARD project, Project number: ZonMW (#73305095007 and Health~Holland, Topsector Life Sciences & Health (PPP-allowance; #LSHM20106).

AMD, CT, JJMvD and MAB report inventorship of the patent “Means and methods for multiparameter cytometry-based leukocyte subsetting” (NL2844751, PCT/NL2020/050688, filing date 5 November 2019), owned by the EuroFlow Consortium. In addition, JJMvD reports to be chairman of the EuroFlow scientific foundation, which receives royalties from licensed patents, which are collectively owned by the participants of the EuroFlow Foundation. These royalties are exclusively used for continuation of the EuroFlow collaboration and sustainability of the EuroFlow consortium. JJMvD reports an Educational Services Agreement from BD Biosciences (San José, CA) and a Scientific Advisor Agreement with Cytognos; all related fees and honoraria are for the Immunology department at Leiden University Medical Center. All other authors declare they have no competing interests.

Authors’ contributions: Conceptualization, HH, JJMvD; Data curation, DH,

LL, SR, AMD; Formal analysis, BN, BdM, RJG, AAV, MdJ, CT, MAB, AMD; Funding acquisition, HH; Investigation, BN, BdM, RJG, IFL, AAV, MdJ, AMD; Methodology, CT; Project administration, DH, LL, AMD; Resources; DH, LL, SR, HH; supervision, HH, JJMvD, MAB, CT; Visualization, AMD; writing – original draft preparation, MAB, AMD; writing – review and editing, all authors read the manuscript, provided feedback and agree with the final manuscript.

Acknowledgments: The authors would like to thank the participants of the 100-plus Study and their family members for providing the blood samples analyzed in this work. Further, we thank the LUMC Vrijwillige Donoren Service (LuVDS), who provided healthy blood samples for optimization of all assays, E. Simonetti (Radboudumc, Laboratory of Medical Immunology) for running the multiplex immunoassay, and the LUMC technical support team for the design and production of the tube heating device used in this study. The authors gratefully acknowledge the Flow cytometry Core Facility at LUMC (coordinated by M. Hameetman, run by operators S. van de Pas, D. Lowie, IJ. Reyneveld and former FCF members dr. K. Schepers, J. Jansen, E. de Haas, and G. de Roo) for their support.

Supplementary Materials: The Supplementary Material for this article can be found online at: https://assets.researchsquare.com/files/rs-1929710/v1/107d2012-dd37-43b1-b2cb-966265d906bf.pdf?c=1661362356

Or using the following QR code:

References

1. Castelo-Branco C, Soveral I. The immune system and aging: a review. Gynecological Endocrinology. 2014;30(1):16-22.
2. Franceschi C, Bonafè M, Valensin S, Olivieri F, De Luca M, Ottaviani E, De Benedictis G. Inflamm-aging: an evolutionary perspective on immunosenescence. Annals of the new York Academy of Sciences. 2000;908(1):244-54.
3. Cancro MP, Hao Y, Scholz JL, Riley RL, Frasca D, Dunn-Walters DK, Blomberg BB. B cells and aging: molecules and mechanisms. Trends in immunology. 2009;30(7):313-8.
4. Frasca D, Diaz A, Romero M, Garcia D, Blomberg BB. B cell immunosenescence. Annual review of cell developmental biology. 2020;36:551-74.
5. Fortin CF, McDonald PP, Lesur O, Fülöp Jr T. Aging and neutrophils: there is still much to do. Rejuvenation research. 2008;11(5):873-82.
6. McLachlan JA, Serkin CD, Morrey KM, Bakouche O. Antitumoral properties of aged human monocytes. The Journal of Immunology. 1995;154(2):832-43.
7. Hearps AC, Martin GE, Angelovich TA, Cheng WJ, Maisa A, Landay AL, Jaworowski A, Crowe SM. Aging is associated with chronic innate immune activation and dysregulation of monocyte phenotype and function. Aging cell. 2012;11(5):867-75.
8. Sims R, Van Der Lee SJ, Naj AC, Bellenguez C, Badarinarayan N, Jakobsdottir J, Kunkle BW, Boland A, Raybould R, Bis JC. Rare coding variants in PLCG2, ABI3, and TREM2 implicate microglial-mediated innate immunity in Alzheimer's disease. Nature

genetics. 2017;49(9):1373-84.
9. van der Lee SJ, Conway OJ, Jansen I, Carrasquillo MM, Kleineidam L, van den Akker E, Hernández I, Van Eijk KR, Stringa N, Chen JAJAn. A nonsynonymous mutation in PLCG2 reduces the risk of Alzheimer's disease, dementia with Lewy bodies and frontotemporal dementia, and increases the likelihood of longevity. 2019;138(2):237-50.
10. Wagner K-H, Cameron-Smith D, Wessner B, Franzke BJN. Biomarkers of aging: from function to molecular biology. 2016;8(6):338.
11. Wilde JI, Watson SP. Regulation of phospholipase C γ isoforms in haematopoietic cells: why one, not the other? Cellular signalling. 2001;13(10):691-701.
12. Wang D, Feng J, Wen R, Marine J-C, Sangster MY, Parganas E, Hoffmeyer A, Jackson CW, Cleveland JL, Murray PJ. Phospholipase Cγ2 is essential in the functions of B cell and several Fc receptors. Immunity. 2000;13(1):25-35.
13. Takalo M, Wittrahm R, Wefers B, Parhizkar S, Jokivarsi K, Kuulasmaa T, Mäkinen P, Martiskainen H, Wurst W, Xiang XJMn. The Alzheimer's disease-associated protective Plcγ2-P522R variant promotes immune functions. 2020;15(1):1-14.
14. Andreone BJ, Przybyla L, Llapashtica C, Rana A, Davis SS, van Lengerich B, Lin K, Shi J, Mei Y, Astarita GJNN. Alzheimer's-associated PLCγ2 is a signaling node required for both TREM2 function and the inflammatory response in human microglia. 2020;23(8):927-38.
15. Strickland SL, Morel H, Prusinski C, Allen M, Patel TA, Carrasquillo MM, Conway OJ, Lincoln SJ, Reddy JS, Nguyen TJAnc. Association of ABI3 and PLCG2 missense variants with disease risk and neuropathology in Lewy body disease and progressive supranuclear palsy. 2020;8(1):1-12.
16. Chen F, Zhang Y, Wang L, Wang T, Han Z, Zhang H, Gao S, Hu Y, Liu GJJoAsD. PLCG2 rs72824905 Variant Reduces the Risk of Alzheimer's Disease and Multiple Sclerosis. 2021(Preprint):1-7.
17. Kleineidam L, Chouraki V, Próchnicki T, van der Lee SJ, Madrid-Marquez L, Wagner-Thelen H, Karaca I, Weinhold L, Wolfsgruber S, Boland A. PLCG2 protective variant p. P522R modulates tau pathology and disease progression in patients with mild cognitive impairment. Acta neuropathologica. 2020;139(6):1025-44.
18. Magno L, Lessard CB, Martins M, Lang V, Cruz P, Asi Y, Katan M, Bilsland J, Lashley T, Chakrabarty PJAsr, therapy. Alzheimer's disease phospholipase C-gamma-2 (PLCG2) protective variant is a functional hypermorph. 2019;11(1):16.
19. Maguire E, Menzies GE, Phillips T, Sasner M, Williams HM, Czubala MA, Evans N, Cope EL, Sims R, Howell GRJTEj. PIP2 depletion and altered endocytosis caused by expression of Alzheimer's disease-protective variant PLCγ2 R522. 2021;40(17):e105603.
20. Holstege H, Beker N, Dijkstra T, Pieterse K, Wemmenhove E, Schouten K, Thiessens L, Horsten D, Rechtuijt S, Sikkes SJEjoe. The 100-plus Study of cognitively healthy centenarians: rationale, design and cohort description. 2018;33(12):1229-49.
21. Tesi N, van der Lee SJ, Hulsman M, Jansen IE, Stringa N, van Schoor N, Meijers-Heijboer H, Huisman M, Scheltens P, Reinders MJJEJoHG. Centenarian controls increase variant effect sizes by an average twofold in an extreme case–extreme control analysis of Alzheimer's disease. 2019;27(2):244-53.
22. Kalina T, Flores-Montero J, Lecrevisse Q, Pedreira CE, Velden VH, Novakova M, Mejstrikova E, Hrusak O, Böttcher S, Karsch D. Quality assessment program for EuroFlow protocols: Summary results of four-year (2010–2013) quality assurance rounds. Cytometry Part A. 2015;87(2):145-56.
23. Kalina T, Flores-Montero J, Van Der Velden V, Martin-Ayuso M, Böttcher S, Ritgen M, Almeida J, Lhermitte L, Asnafi V, Mendonca A. EuroFlow standardization of flow cytometer instrument settings and immunophenotyping protocols. Leukemia. 2012;26(9):1986-2010.

24. Pan Kvd, Bruin-Versteeg Sd, Damasceno D, Hernández-Delgado A, Sluijs-Gelling AJvd, Bossche WBvd, Laat IFd, Diez P, Naber BA, Diks AM, Berkowska MA, Mooij Bd, Groenland RJ, Bie FJd, Khatri I, Kassem S, Jager ALd, Louis A, Almeida J, Gaans Jv, Barkoff A-M, He Q, Ferwerda G, Versteegen P, Berbers GA, Orfao A, Dongen JJMv, Teodosio C. Development of a standardized and validated flow cytometry approach for monitoring of innate myeloid immune cells in human blood. in review at Frontiers at Immunology. 2022.
25. van Dongen JJMOdMCEV, J.A. ; Goncalves Grunho Teodosio, C.I.; Perez Y Andres, M.; Almeida Parra, J.M.; Van den Bossche, W.B.L.; Botafogo Goncalves, V.D.; Berkowska, M.A.; Van der Pan, K.; Blanco Alvarez, E.; Diks, A.M. , inventor; P119646NL00, assignee. Means and methods for multiparameter cytometry-based leukocyte subsetting. The Netherlands2019 priority date 5 November 209.
26. Botafogo V, Pérez-Andres M, Jara-Acevedo M, Bárcena P, Grigore G, Hernández-Delgado A, Damasceno D, Comans S, Blanco E, Romero A. Age Distribution of Multiple Functionally Relevant Subsets of CD4+ T Cells in Human Blood Using a Standardized and Validated 14-Color EuroFlow Immune Monitoring Tube. Frontiers in Immunology. 2020;11:166.
27. Blanco E, Pérez-Andrés M, Arriba-Méndez S, Contreras-Sanfeliciano T, Criado I, Pelak O, Serra-Caetano A, Romero A, Puig N, Remesal A. Age-associated distribution of normal B-cell and plasma cell subsets in peripheral blood. Journal of Allergy and Clinical Immunology. 2018;141(6):2208-19. e16.
28. Diks AM, Versteegen P, Teodosio C, Groenland RJ, de Mooij B, Buisman A-M, Torres-Valle A, Pérez-Andrés M, Orfao A, Berbers GAM, van Dongen JJM, Berkowska MA, Consortium obotI-P. Age and Primary Vaccination Background Influence the Plasma Cell Response to Pertussis Booster Vaccination. 2022;10(2):136.
29. Darrah PA, Patel DT, De Luca PM, Lindsay RW, Davey DF, Flynn BJ, Hoff ST, Andersen P, Reed SG, Morris SL. Multifunctional TH 1 cells define a correlate of vaccine-mediated protection against Leishmania major. Nature medicine. 2007;13(7):843-50.
30. Van Zelm MC, Van Der Burg M, Langerak AW, Van Dongen JJ. PID comes full circle: applications of V (D) J recombination excision circles in research, diagnostics and newborn screening of primary immunodeficiency disorders. Frontiers in immunology. 2011;2:12.
31. Van Zelm MC, Szczepański T, Van Der Burg M, Van Dongen JJ. Replication history of B lymphocytes reveals homeostatic proliferation and extensive antigen-induced B cell expansion. The Journal of experimental medicine. 2007;204(3):645-55.
32. Fröberg J, Gillard J, Philipsen R, Lanke K, Rust J, van Tuijl D, Teelen K, Bousema T, Simonetti E, van der Gaast-de Jongh CJNc. SARS-CoV-2 mucosal antibody development and persistence and their relation to viral load and COVID-19 symptoms. 2021;12(1):1-11.
33. Garner C, Tatu T, Reittie J, Littlewood T, Darley J, Cervino S, Farrall M, Kelly P, Spector T, Thein SJB, The Journal of the American Society of Hematology. Genetic influences on F cells and other hematologic variables: a twin heritability study. 2000;95(1):342-6.
34. Hall M, Ahmadi K, Norman P, Snieder H, MacGregor A, Vaughan R, Spector T, Lanchbury JJG, Immunity. Genetic influence on peripheral blood T lymphocyte levels. 2000;1(7):423-7.
35. Kurosaki T, Aiba Y, Kometani K, Moriyama S, Takahashi YJIr. Unique properties of memory B cells of different isotypes. 2010;237(1):104-16.
36. Kolibab K, Smithson SL, Rabquer B, Khuder S, Westerink MJJI, immunity. Immune response to pneumococcal polysaccharides 4 and 14 in elderly and young adults: analysis of the variable heavy chain repertoire. 2005;73(11):7465-76.
37. Ademokun A, Wu YC, Martin V, Mitra R, Sack U, Baxendale H, Kipling D, Dunn-Walters DKJAc. Vaccination-induced changes in human B-cell repertoire and pneu-

mococcal IgM and IgA antibody at different ages. 2011;10(6):922-30.
38. Spiegelberg H, Melewicz F, Ferreri N, editors. IgE Fc receptors on monocytes and allergy. Annales de l'Institut Pasteur/Immunologie; 1986: Elsevier.
39. Plaut M, Pierce JH, Watson CJ, Hanley-Hyde J, Nordan RP, Paul WEJN. Mast cell lines produce lymphokines in response to cross-linkage of FcεRI or to calcium ionophores. 1989;339(6219):64-7.
40. Gould HJ, Sutton BJJNRI. IgE in allergy and asthma today. 2008;8(3):205-17.
41. Jiang T, Yu J-T, Hu N, Tan M-S, Zhu X-C, Tan LJMn. CD33 in Alzheimer's disease. 2014;49(1):529-35.
42. Bradshaw EM, Chibnik LB, Keenan BT, Ottoboni L, Raj T, Tang A, Rosenkrantz LL, Imboywa S, Lee M, Von Korff AJNn. CD33 Alzheimer's disease locus: altered monocyte function and amyloid biology. 2013;16(7):848-50.
43. Fülöp Jr T, Foris G, Worum I, Leövey A. Age-dependent alterations of Fc gamma receptor-mediated effector functions of human polymorphonuclear leucocytes. Clinical and experimental immunology. 1985;61(2):425.
44. Butcher S, Chahal H, Nayak L, Sinclair A, Henriquez N, Sapey E, O'mahony D, Lord J. Senescence in innate immune responses: reduced neutrophil phagocytic capacity and CD16 expression in elderly humans. Journal of leukocyte biology. 2001;70(6):881-6.
45. Gabandé-Rodríguez E, Keane L, Capasso MJJonr. Microglial phagocytosis in aging and Alzheimer's disease. 2020;98(2):284-98.
46. Guen YL, Luo G, Ambati A, Damotte V, Jansen I, Yu E, Nicolas A, de Rojas I, Leal TP, Miyashita A, Bellenguez C, Lian MM, Parveen K, Morizono T, Park H, Grenier-Boley B, Naito T, Küçükali F, Talyansky SD, Yogeshwar SM, Sempere V, Satake W, Alvarez V, Arosio B, Belloy ME, Benussi L, Boland A, Borroni B, Bullido MJ, Caffarra P, Clarimon J, Daniele A, Darling D, Debette S, Deleuze J-F, Dichgans M, Dufouil C, During E, Düzel E, Galimberti D, Garcia-Ribas G, García-Alberca JM, García-González P, Giedraitis V, Goldhardt O, Graff C, Grünblatt E, Hanon O, Hausner L, Heilmann-Heimbach S, Holstege H, Hort J, Jung YJ, Jürgen D, Kern S, Kuulasmaa T, Ling L, Masullo C, Mecocci P, Mehrabian S, de Mendonça A, Boada M, Mir P, Moebus S, Moreno F, Nacmias B, Nicolas G, Nordestgaard BG, Papenberg G, Papma J, Parnetti L, Pasquier F, Pastor P, Peters O, Pijnenburg YAL, Piñol-Ripoll G, Popp J, Porcel LM, Puerta R, Pérez-Tur J, Rainero I, Ramakers I, Real LM, Riedel-Heller S, Rodriguez-Rodriguez E, Luís Royo J, Rujescu D, Scarmeas N, Scheltens P, Scherbaum N, Schneider A, Seripa D, Skoog I, Solfrizzi V, Spalletta G, Squassina A, van Swieten J, Sánchez-Valle R, Tan E-K, Tegos T, Teunissen C, Thomassen JQ, Tremolizzo L, Vyhnalek M, Verhey F, Waern M, Wiltfang J, Zhang J, Zetterberg H, Blennow K, Williams J, Amouyel P, Jessen F, Kehoe PG, Andreassen O, Van Duin C, Tsolaki M, Sánchez-Juan P, Frikke-Schmidt R, Sleegers K, Toda T, Zettergren A, Ingelsson M, contributors E, group GAs, consortium D, DemGene, EADI, GERAD, consortium APsDG, Okada Y, Rossi G, Hiltunen M, Gim J, Ozaki K, Sims R, Foo JN, van der Flier W, Ikeuchi T, Ramirez A, Mata I, Ruiz A, Gan-Or Z, Lambert J-C, Greicius MD, Mignot E. Protective association of HLA-DRB1*04 subtypes in neurodegenerative diseases implicates acetylated Tau PHF6 sequences. 2021:2021.12.26.21268354.
47. Phongpreecha T, Fernandez R, Mrdjen D, Culos A, Gajera CR, Wawro AM, Stanley N, Gaudilliere B, Poston KL, Aghaeepour N. Single-cell peripheral immunoprofiling of Alzheimer's and Parkinson's diseases. Science advances. 2020;6(48):eabd5575.
48. D'Andrea MR, Cole GM, Ard MDJNoa. The microglial phagocytic role with specific plaque types in the Alzheimer disease brain. 2004;25(5):675-83.
49. Britschgi M, Olin C, Johns H, Takeda-Uchimura Y, LeMieux M, Rufibach K, Rajadas J, Zhang H, Tomooka B, Robinson W. Neuroprotective natural antibodies to assemblies of amyloidogenic peptides decrease with normal aging and advancing Alzheimer's disease. Proceedings of the National Academy of Sciences. 2009;106(29):12145-50.

50. Rosenmann H, Meiner Z, Geylis V, Abramsky O, Steinitz M. Detection of circulating antibodies against tau protein in its unphosphorylated and in its neurofibrillary tangles-related phosphorylated state in Alzheimer's disease and healthy subjects. Neuroscience letters. 2006;410(2):90-3.
51. Sevigny J, Chiao P, Bussière T, Weinreb PH, Williams L, Maier M, Dunstan R, Salloway S, Chen T, Ling Y. The antibody aducanumab reduces Aβ plaques in Alzheimer's disease. Nature immunology. 2016;537(7618):50-6.
52. Tolar M, Abushakra S, Hey JA, Porsteinsson A, Sabbagh M. Aducanumab, gantenerumab, BAN2401, and ALZ-801—the first wave of amyloid-targeting drugs for Alzheimer's disease with potential for near term approval. Alzheimer's research therapy. 2020;12(1):1-10.
53. Congdon EE, Sigurdsson EM. Tau-targeting therapies for Alzheimer disease. Nature Reviews Neurology. 2018;14(7):399-415.